ELSEVIER

Catalysis Today 67 (2001) 369–378

CATALYSIS TODAY

www.elsevier.com/locate/cattod

Fundamental and combinatorial approaches in the search for and optimisation of catalytic materials for the oxidative dehydrogenation of propane to propene

O.V. Buyevskaya, A. Brückner,
E.V. Kondratenko, D. Wolf, M. Baerns*

Institute for Applied Chemistry Berlin-Adlershof (ACA), Richard-Willstätter-Str. 12, D-12489 Berlin, Germany

Abstract

An evolutionary approach was applied to create five generations of α-Al_2O_3-supported multi-metal-oxides to be used as catalytic materials for the oxidative dehydrogenation of propane at 773 K. Each generation consisted of 56 differently composed materials, i.e., a total amount of 280 materials. These catalytic materials were tested in parallel. For the best materials propene yields from 7% (1st generation) to 9% (5th generation) were achieved. Some of these superior catalysts were characterised by XRD, XPS and EPR. A correlation between catalytic performance and the Mg/V ratio on the surface was found. Based on the structural knowledge obtained, from which the requirement of isolated or at least weakly interacting vanadium sites was derived, VO_x (2.8 wt.%)/MCM-48 and VO_x (2.8 wt.%)/MCM-41 catalysts with a high dispersion of vanadia were used as reference giving a maximal propene yield of 17 and 15%, respectively. © 2001 Elsevier Science B.V. All rights reserved.

Keywords: Combinatorial catalysis; Evolutionary catalyst optimization approach; Propane oxidative dehydrogenation; Solid mixed metal oxides

1. Introduction

The development of new catalytic materials occurs still mainly on an empirical basis although significant progress has been made in the fundamental understanding of catalysis. Nevertheless, it is still not possible to design a catalyst “ab initio” predicting its required composition and its resulting activity and selectivity for a given reaction; this is particularly true for heterogeneous multi-compound catalysts.

We have recently suggested a combinatorial approach including an evolutionary optimisation procedure for finding new or improved catalytic materials [1,2]. Fundamental pre-knowledge is applied for defining a pool of elements (or compounds) from which a 1st generation of numerous materials is prepared by randomisation of their qualitative and quantitative composition. The evolutionary procedure consisting of mutation and cross-over processes is then applied to prepare subsequent generations based on the catalytic performance of the materials of the preceding generation; a genetic algorithm with the ability to search a large parameter space in a highly directed way was used for the mathematical treatment of the procedure.

By using high-throughput testing and parallel synthesis a large number of different materials can be prepared and tested in a relatively short time compared

---

* Corresponding author. Tel.: +49-30-6392-4444;
fax: +49-30-6392-4454.
E-mail address: baerns@aca-berlin.de (M. Baerns).

PII: S0920-5861(01)00329-7

to conventional methods. Several applications of the high-throughput techniques have been reported for the development of solid materials (see e.g. [3–7]).

The aim of the present contribution is to illustrate how the fundamental knowledge is used in designing the 1st generation by the above-described procedure; the best materials obtained after a series of generations are then improved based on fundamental insights derived from their characterisation using classical methods of preparation of catalytic materials. This is outlined in the search for and optimisation of catalysts for the oxidative dehydrogenation of propane (ODP). This reaction was chosen as a model reaction since we were interested to learn whether the applied combinatorial procedure, which was only based on some general pre-knowledge on partial hydrocarbon oxidation, would lead to similar results.

Numerous multi-component oxide materials have been developed for the transformation of alkanes into desired products [8–12]. In a more general sense, the catalytic surface process, which may lead to propene formation in ODP can be classified according to the following assumptions:

- participation of removable lattice oxygen (redox-type catalysts);
- participation of adsorbed oxygen;
- participation of non-removable lattice oxygen.

Our methodology in applying fundamental knowledge in the evolutionary procedure and in optimising the "best" catalytic materials obtained hereby is described below. Since this work aimed at proofing the principle it should not be surprising that materials are found which have already been discovered earlier.

2. Methodology

2.1. Pre-selection of individual compounds

Based upon the three assumed reaction mechanisms (see above), eight individual metal oxides were selected:

- redox properties: V_2O_5, MoO_3, MnO_2, Fe_2O_3, Ga_2O_3;
- dissociative adsorbed oxygen: La_2O_3;
- non-removable lattice oxygen: B_2O_3, MgO.

By arbitrary decision all the materials of the 1st generation consisted of only four individual metal oxides deposited on α-alumina. The composition of the various materials of the 1st generation was reported earlier [1]. The compositions of the subsequent four generations were always defined by the catalytic performance of the materials of the preceding generation whereby emphasis was put on the composition of the best performing materials [1].

2.2. Feed back of characterisation results of catalytic materials for further optimisation

For materials of significantly good catalytic performances XRD was applied for identifying phase compositions. The composition space, which appeared attractive for further improvement, was more deeply studied. Furthermore, the surfaces and the bulk of the materials were characterised by UV/Vis and EPR.

3. Experimental

3.1. Catalyst preparation

Most of the materials were prepared manually, more recently the preparation can also be done automatically applying a SOPHAS robot, the operation of which and reproducibility of catalytic materials will be explained separately. For preparing catalytic materials, the following compounds were used: NH_4VO_3 (Merck, p.a.), $Mg(NO_3)_2 \cdot 4H_2O$ (Merck, p.a.), H_3BO_3 (Merck, p.a.), $(NH_4)_6Mo_7O_{24} \cdot 4H_2O$ (Riedel de Haën, p.a.), $La(NO_3)_2 \cdot 6H_2O$ (Merck, p.a.), $Mn(NO_3)_2 \cdot 4H_2O$ (Merck, p.a.), $Fe(NO_3)_3 \cdot 9H_2O$ (Fluka, p.a.), $Ga(NO_3)_3 \cdot 6H_2O$ (Alfa, 99.9%). These primary compounds were dispersed or dissolved in water in the presence of granulated α-Al_2O_3 (CONDEA, particle size: $d_p = 1\,mm$, $S_{BET} = 5\,m^2/g$) which served as an inert support of the active mass amounting to 30 wt.%. The volume of the aqueous solution used per gram of support was 10 ml. The mixture was stirred for 30 min at 80°C. The excess water was evaporated while stirring at ca. 100°C; the remaining solid was then dried at 120°C for 10 h and finally calcined at 600°C for 3 h in air. Furthermore, a ternary V–Mg–Ga oxides library was similarly prepared. For preparation of two binary V–Ga and V–Mg oxide materials Ga_2O_3 or $Mg(OH)_2$ was added to a water solution of NH_4VO_3 (Merck, p.a.) followed by water evaporation, drying and final calcination at 600°C for 3 h in air.

3.2. Catalyst characterisation

Specific surface areas of the catalysts were determined by the one-point BET method using Gemini III equipment (Micromeritics).

XRD powder analyses were carried out using a STADIP transmission powder diffractometer (Stoe) with Cu $K\alpha_1$ radiation.

EPR spectra were acquired with an ELEXSYS 500-10/12 (Bruker) spectrometer in X-band at both 298 and 77 K. The magnetic field was measured with respect to the standard 2,2-diphenyl-1-picrylhydrazyl hydrate (DPPH).

UV/Vis–DRS measurements were performed using a Cary 400 UV/Vis spectrometer (Varian) equipped with a diffuse reflectance accessory (praying mantis, Harrick). The reflectance spectra were converted into the Kubelka–Munk function $F(R)$ which is proportional to the absorption coefficient for low values of $F(R)$. Spectra were deconvoluted into Gaussian bands using the GRAMS/386 program (Galactic Industries).

The near-surface composition of catalysts was derived from XPS spectra recorded with an ESCALAB-220i-XL (Fisons Instruments) using Al $K\alpha$ radiation (1486.6 eV).

3.3. Catalytic testing

The catalytic tests were carried out at ambient pressure in U-form fixed-bed quartz reactors operating in parallel which were immersed into a bed of fluidised sand serving as a source or sink of heat; hereby isothermal operation was achieved. The feed consisted of oxygen, propane and nitrogen; the mixtures applied amounted to: $C_3H_8/O_2/N_2 = 30/10/60$ or $C_3H_8/O_2/N_2 = 40/20/40$ vol.%. For acquiring selectivities at different degrees of propane conversion the total flow rate was varied from 10 to 150 cm^3/min per reactor which was charged with 300 mg of catalytic material. The reaction temperature was fixed at 773 K. The products and reactants were analysed by using a gas chromatograph (Satochrom) equipped with Poraplot Q and Molesieve 5 columns.

4. Results and discussion

4.1. Catalytic performances

For oxidative dehydrogenation of propane catalytic materials of different compositions were studied at 773 K. The catalysts can be classified into five groups based on their chemical composition and preparation method:

Evolutionary method
  1st group: 56 catalytic materials in each generation amounting to a total number of 280 for five generations.
Further optimisation of best performing materials (non-combinatorial approach)
  2nd group: 36 V–Mg–Ga–O/α-Al_2O_3 combinations;
  3rd group: 11 V–Ga–O combinations;
  4th group: 4 V–Mg–O combinations [13];
  5th group: VO_x/MCM-41, VO_x/MCM-48 [14];

The catalytic materials of 1st group were evaluated based on a combinatorial procedure described earlier in detail [1,2]. The chemical composition and catalytic performance of these materials were also reported [1,2]. Based on the catalytic performance of the materials of the 1st generation, the 2nd generation of catalytic materials were produced applying evolutionary operators (mutaion, crossover). According to this procedure, five generations were prepared and tested for ODP in this study. As a result of the evolutionary procedure, an improvement of catalytic performance was found. The materials with which the best propene yields were obtained in each generation are summarised in Fig. 1; the respective compositions are given in Table 1. It should be noted that the degree of oxygen conversion was close to 100% in all these experiments. In Fig. 1, the average performance data of all materials of each generation are presented indicating also an improvement when proceeding from one to the next generation. It is obvious that MgO, V_2O_5, and Ga_2O_3 are the essential compounds of the best materials; however, even the best materials of the 5th generation still contain minor amounts of Fe, Mn,

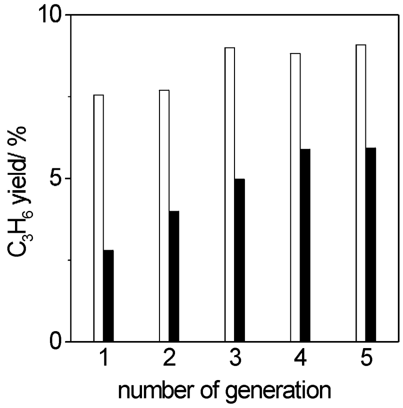

Fig. 1. Best (open bar) and mean yield (solid bar) of propene in each generation ($C_3H_8/O_2/N_2$ = 30/10/60, T = 773 K, $X(O_2) \sim 100\%$).

and Mo, respectively. To exclude the effect of the later three compounds on catalytic performance of the catalysts of 1st group, 36 V–Mg–Ga mixed metal-oxides of different composition supported on α-Al_2O_3 were tested for ODP at 773 K using a reaction mixture of $C_3H_8/O_2/N_2 = 30/10/60$. The best materials along with their performance data are shown in Table 2; for illustration all the yields of all materials are presented in Fig. 2. The propene yields obtained are slightly lower than the results described above which may be due to the absence of Fe, Mn or Mo. Weight concentrations of vanadium (3.5–4.6%) in the superior catalytic materials were close to those in the best materials created by the combinatorial procedure. Decreasing or increasing the vanadium content resulted in a loss of catalytic efficiency.

The two best catalysts from 3rd and 5th generation (1st group) and from the V–Mg–Ga–O library (2nd group), respectively, were chosen to check the effect of oxygen partial pressure on ODP. A $C_3H_8/O_2/N_2 = 2/1/2$ reaction mixture was used. The results obtained and presented in Fig. 3 show that decreases and increases in propene yield vary from −0.59 to +2.17 on increasing oxygen partial pressure from 15 to 20 kPa. The differences found will be discussed in connection with the catalyst composition further below.

For comparison, V–Ga and V–Mg oxides prepared by non-combinatorial approach were tested for ODP to study the effect of MgO or Ga_2O_3 separately on the catalytic performance of vanadia using a reaction mixture of $C_3H_8/O_2/N_2 = 2/1/2$. For the V–Ga oxide systems the catalytic performance, i.e., degree of conversion, selectivity and yield of propene have a maximum at low vanadia content; at V/Ga = 0, however, there is no conversion at all (Fig. 4). A similar effect of vanadia loading was found on VO_x/SiO_2 [15]. In our

Table 1
Performance and composition of the best catalytic materials in each generation along with the contact time for nearly complete oxygen conversion ($C_3H_8/O_2/N_2 = 30/10/60$, T = 773 K, m_{cat} = 300 mg)

Generation No.	Me-oxide composition	τ (s g_{cat} cm^{-3})	$X(C_3H_8)$ (%)	$Y(C_3H_6)$ (%)	$S(C_3H_6)$ (%)
1	$V_{0.25}Mg_{0.52}Ga_{0.11}Mo_{0.12}$	0.12	12.4	7.5	60.4
2	$V_{0.47}Ga_{0.21}Mo_{0.05}Mn_{0.27}$	0.12	14.7	7.7	52.1
3	$V_{0.22}Mg_{0.47}Ga_{0.2}Mo_{0.11}$	0.9	15.7	9.0	57.4
4	$V_{0.27}Mg_{0.37}Ga_{0.11}Mo_{0.12}Fe_{0.13}$	0.12	15.2	8.8	57.9
5	$V_{0.32}Mg_{0.18}Ga_{0.27}Mo_{0.04}Mn_{0.19}$	0.12	16.9	9.0	53.3

Table 2
Performance and composition of the best catalytic materials of V–Mg–Ga library along with the contact time for nearly complete oxygen conversion ($C_3H_8/O_2/N_2 = 30/10/60$, T = 773 K, m_{cat} = 200 mg)

Me-oxide composition	τ (s g_{cat} cm^{-3})	$X(C_3H_8)$ (%)	S(CO_x) (%)	S(C_3H_6) (%)	Y(C_3H_6) (%)
$V_{0.2}Mg_{0.1}Ga_{0.7}$	0.12	16.1	45.9	47.9	7.7
$V_{0.2}Mg_{0.2}Ga_{0.6}$	0.12	16.2	43.9	49.5	8.0
$V_{0.2}Mg_{0.3}Ga_{0.5}$	0.12	16.1	44.2	48.7	7.9
$V_{0.2}Mg_{0.4}Ga_{0.4}$	0.12	16.4	45.1	48.9	8.0
$V_{0.2}Mg_{0.5}Ga_{0.3}$	0.08	16.5	43.2	51.0	8.4

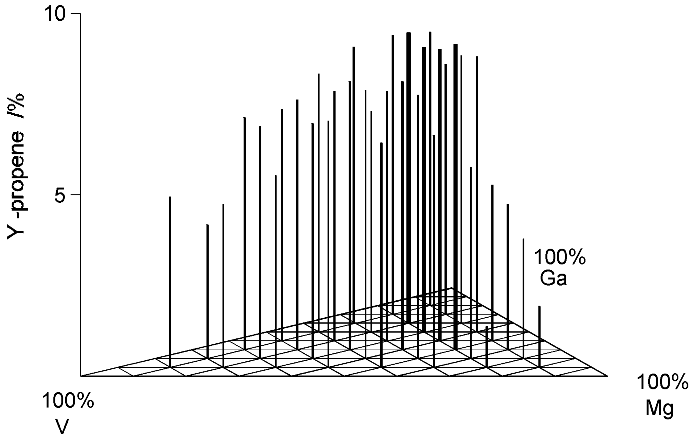

Fig. 2. Catalytic performance of V–Mg–Ga mixed oxides in the oxidative propane dehydrogenation ($C_3H_8/O_2/N_2 = 30/10/60$, $T = 773$ K, $X(O_2) = 20$–100%).

study, the best yields were obtained on materials with a weight concentration of vanadium in the range from 2.6 to 8.3%. Comparing the catalytic performances of the various V–Ga–O compositions with those of the library consisting of 36 V–Mg–Ga–O compositions or the materials from the combinatorial study it turns out that VO_x/Ga_2O_3 catalysts have the lowest selectivity. This means that mainly the presence of magnesium oxide but also possibly of Fe, Mo or Mn is necessary to obtain a good catalytic performance. This important information is a direct result of the combinatorial approach. Fig. 5 shows catalytic performance of V–Mg oxidic systems. Propene yields of up to 13% were achieved. As for V–Ga oxides both selectivity and yield of propene decreased with an increase of vanadia concentration. A composition of $V_{0.1}Mg_{0.9}O_x$ leads to the best catalytic performance.

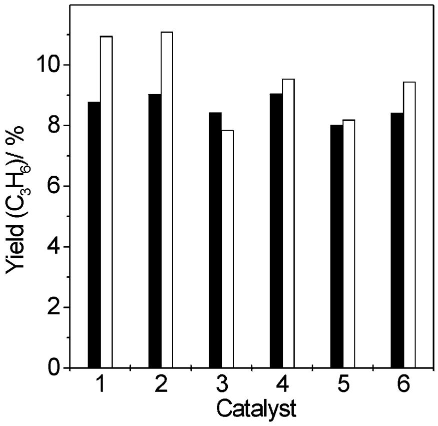

Fig. 3. Yield of propene for the two best-performing catalytic materials from the evolutionary procedure (3rd and 5th generations) and V–Mg–Ga-mixed oxides: (1) $V_{0.3}Mg_{0.63}Ga_{0.07}$; (2) $V_{0.22}Mg_{0.47}Mo_{0.11}Ga_{0.2}$; (3) $V_{0.16}Mg_{0.11}Mo_{0.17}Fe_{0.09}Ga_{0.47}$; (4) $V_{0.32}Mg_{0.18}Mo_{0.04}Mn_{0.19}Ga_{0.27}$; (5) $V_{0.2}Mg_{0.2}Ga_{0.6}$; (6) $V_{0.2}Mg_{0.5}Ga_{0.3}$. Solid bar — $C_3H_8/O_2/N_2 = 30/10/60$, $T = 773$ K, $X(O_2) \sim 100\%$; open bar — $C_3H_8/O_2/N_2 = 40/20/40$, $T = 773$ K, $X(O_2) \sim 100\%$.

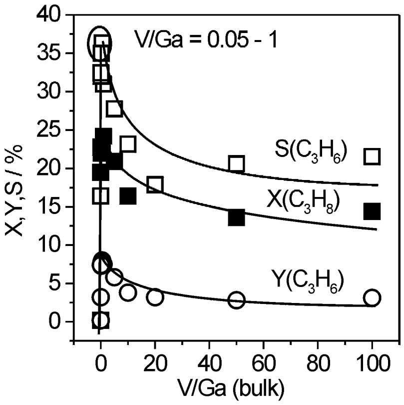

Fig. 4. Catalytic performance of various V–Ga oxides in the oxidative propane dehydrogenation ($C_3H_8/O_2/N_2 = 40/20/40$, $T = 773$ K).

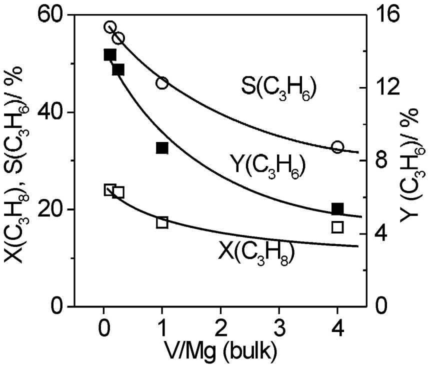

Fig. 5. Catalytic performance of various V–Mg oxides in the oxidative propane dehydrogenation ($C_3H_8/O_2/N_2 = 40/20/40$, $T = 773\,K$, $X(O_2) = 95–100\%$).

4.2. Results on catalyst characterisation

From the above it became obvious that catalytic performance of complex oxide system depends on structural peculiarities of these systems. Therefore, it was of particular interest to characterise systematically the more effective catalysts to derive structural information needed for improving catalyst design. Characterisation results on S_{BET}, paramagnetic VO_x species (EPR), phases (XRD) and surface composition (XPS) are discussed.

Bulk and surface composition as well as surface areas of the best catalytic materials from both combinatorial approach and classical preparation are summarised in Table 3. The materials consisted of both amorphous and crystalline phases. Different crystalline phases were found to depend on chemical composition. For V–Ga oxides only phases of pure oxides (V_2O_5 or Ga_2O_3) were detected. In all V, Mg-containing materials different $Mg_xV_yO_z$ phases were found. These phases differ in Mg/V ratio ranging between 0.5 and 1.5. Differences in the Mg/V ratio derived from XPS were significantly higher (0.2–9.3). This ratio is assumed to reflect the surface distribution of vanadia; the higher the ratio, the lower the concentration of closely associated vanadia sites.

The catalysts $V_{0.8}Mg_{0.2}O_x$ and $V_{0.1}Mg_{0.9}O_x$ which are associated with the highest and lowest propene yields, respectively (Table 3), have been studied by EPR and UV/Vis diffuse reflectance spectroscopy to gain information on the degree of vanadium-site isolation [13]. The UV/Vis spectrum of sample $V_{0.8}Mg_{0.2}O_x$ (Fig. 6(B)) shows the typical charge-transfer (CT) bands of pentavalent vanadyl species in crystalline V_2O_5 [16]. This is in agreement with XRD results which confirm the presence of V_2O_5 as the main component in $V_{0.8}Mg_{0.2}O_x$. The mean vanadium valence state determined by potentiometric titration [17] amounts to 4.912 indicating that 8.2% of all vanadium ions are tetravalent. This percentage is too small to be detected in the UV/Vis spectra besides V^{5+}. However, the EPR spectrum in which only tetravalent vanadium ions can be detected under the recording conditions applied, shows a narrow isotropic singlet (Fig. 7) which is characteristic of

Table 3
Results of bulk and surface characterisation and catalytic performance ($T = 773\,K$, $C_3H_8/O_2/N_2 = 40/20/40$)

Oxide materials	S_{BET} (m^2/g)	Crystalline phases (XRD)	Mg/V, Ga/V (XPS)	τ ($s\,g\,cm^{-3}$)	$S(C_3H_6)$ (%)	$X(C_3H_8)$ (%)
$V_{0.3}Mg_{0.63}Ga_{0.07}$	10	$Mg_2V_2O_7$	2	0.18	49	22.4
$V_{0.22}Mg_{0.47}Mo_{0.11}Ga_{0.2}$	17	$Mg_2V_2O_7$	3.33	0.30	49.7	22.3
$V_{0.32}Mg_{0.18}Mo_{0.04}Mn_{0.19}Ga_{0.33}$	13	MgV_2O_6, $Mn(VO_3)_2$, $Mn(V_2O_7)$	0.47	0.12	40.3	19.5
$V_{0.16}Mg_{0.11}Mo_{0.17}Fe_{0.09}Ga_{0.47}$	14	Ga_2O_3, $FeVO_4$, MoO_3, $FeGa_2O_4$	0.21	0.08	45.2	21.1
$V_{0.2}Mg_{0.2}Ga_{0.6}$	13.5	MgV_2O_6, Ga_2O_3, V_2O_4	0.34	0.12	42.1	19.5
$V_{0.2}Mg_{0.5}Ga_{0.3}$	14.1	$Mg_3(VO_4)_2$, V_2O_4, $Mg_xV_yO_z$	0.5	0.06	45.4	20.8
$V_{0.8}Mg_{0.2}$	1.9	V_2O_5, MgV_2O_6	0.2	0.80	32.8	16.3
$V_{0.5}Mg_{0.5}$	7.9	$Mg_2V_2O_7$	1.2	1.20	46	18.9
$V_{0.2}Mg_{0.8}$	46.9	$Mg_3V_2O_8$, MgO	4.5	0.24	55.2	23.6
$V_{0.1}Mg_{0.9}$	87.4	$Mg_3V_2O_8$, MgO	9.3	0.24	57.5	24
$V_{0.5}Ga_{0.5}$	7.2	V_2O_5, Ga_2O_3	2.1	0.18	31	24.2
$V_{0.33}Ga_{0.67}$	4.9	V_2O_5, Ga_2O_3	0.91	0.18	36.4	22
$V_{0.16}Ga_{0.84}$	4.8	V_2O_5, Ga_2O_3	0.63	0.18	35	22

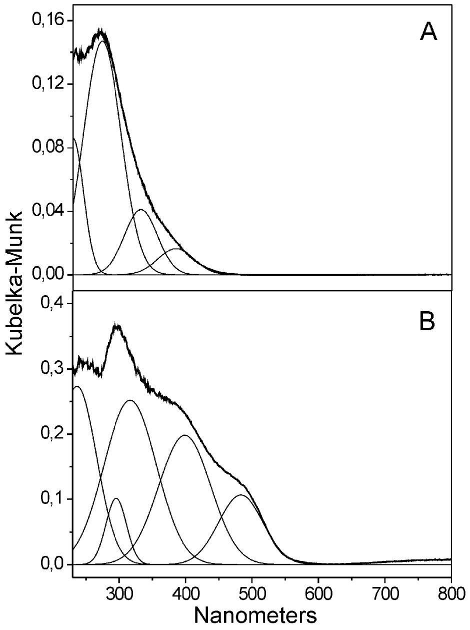

Fig. 6. UV/Vis–DRS spectra of the catalysts $V_{0.1}Mg_{0.9}O_x$ (A) and $V_{0.8}Mg_{0.2}O_x$ (B).

closely neighbouring VO^{2+} ions coupled by effective spin–spin exchange interactions [18]. These species are most likely formed by partial reduction of V_2O_5. Thus, as a rough approximation, the distribution of tetravalent vanadium sites reflected by EPR can be taken as a monitor for the distribution of VO^{3+}, too.

In the UV/Vis spectrum of sample $V_{0.1}Mg_{0.9}O_x$ CT bands of isolated tetrahedral V^{5+} [16] can be identified by spectra deconvolution at 224, 268 and 326 nm (Fig. 6(A)). They arise most likely from magnesium orthovanadate detected, besides MgO, as a minor component in this catalyst by XRD. Additionally, a weak band at 380 nm points to the presence of some V^{5+} in isolated octahedral or square–pyramidal coordination [19]. The EPR spectrum of $V_{0.1}Mg_{0.9}O_x$ shows the characteristic hyperfine splitting (hfs) multiplet of well-isolated octahedrally coordinated VO^{2+} species [20] superimposed on a broad isotropic singlet of weakly interacting VO^{2+} species (Fig. 7). By spectra simulation it has been derived that the latter comprise about 97% of the overall EPR active V^{4+} content. Those species are probably isolated dispersed on the surface of MgO being the main component in $V_{0.1}Mg_{0.9}O_x$. In contrast to sample $V_{0.8}Mg_{0.2}O_x$ in which a narrow EPR singlet arises from effective spin–spin exchange interactions between closely neighbouring VO^{2+} sites, the mutual distance of these species in sample $V_{0.1}Mg_{0.9}O_x$ should be markedly longer since the large line width of the isotropic EPR singlet suggests weak dipolar interactions only. This is confirmed, too, by the UV/Vis spectrum (Fig. 6(A)) in which no bands of oligomeric $V^{5+}O_x$ units at wavelength higher than 390 nm are observed. Thus, all vanadium species in sample $V_{0.1}Mg_{0.9}O_x$ including those giving rise to the broad EPR singlet can be regarded as more or less isolated insofar as they do most probably not form V–O–V bonds.

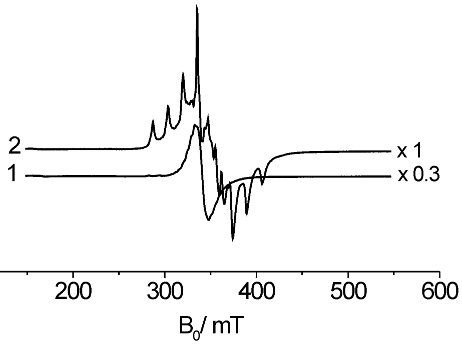

Fig. 7. EPR Spectra at $T = 77\,K$ of $V_{0.8}Mg_{0.2}O_x$ (1) and $V_{0.1}Mg_{0.9}O_x$ (2).

The EPR spectra of catalytic materials with vanadium contents between those of $V_{0.1}Mg_{0.9}O_x$ and $V_{0.8}Mg_{0.2}O_x$ ($3.3 < V\,content/wt.\% < 15$) show also a superposition of an hfs multiplet of isolated VO^{2+} species and a more or less broad isotropic singlet of interacting VO^{2+} species. With increasing vanadium concentration the fraction of interacting vanadyl species increases.

4.3. Dependence of catalytic properties on structural characterisation and further improvement of the catalytic material

The results on catalyst characterisation are discussed to explain the catalytic performance of the various best performing materials (groups 1–4) for which data are presented in Table 3. In all the experiments reported the degree of oxygen conversion amounted to 100% or was close to this value (>95%).

The materials differed both in selectivity and yield of propene. $V_{0.8}Mg_{0.2}$ and all V–Ga–O materials have the lowest selectivity and yield of propene. For these materials a pure V_2O_5 phase was detected by XRD. In general, supported catalysts with high concentration of vanadia or bulk V_2O_5 are not selective for propane oxidation as has been shown previously [15,21]. This was explained by the acceleration of non-selective propene oxidation due to the presence of neighbouring vanadia species. The present study showed that vanadium oxide is agglomerated in $V_{0.8}Mg_{0.2}O_x$. The surface dispersion of vanadia as determined by XPS is also low in comparison to other V–Mg oxides materials containing less bulk vanadium. For the materials with low vanadium content, no formation of crystalline V_2O_5 was observed (Table 3); different $V_xMg_yO_z$ phases were detected. In literature [21–23], there are contradictory conclusions concerning the active phases responsible for olefin formation. In our case XPS data show that the materials differ strongly in surface dispersion of vanadia which is determined by the surface ratio of Mg/V (Table 3). If the distribution of vanadia species does play the important role in ODP the catalytic performance should depend on the Mg/V ratio. Fig. 8 shows this correlation; an increase in propene yield is achieved by increasing the Mg/V ratio. The increase of propene yield can be explained by the fact that the non-selective oxidation of propene to CO_x is inhibited with decreasing the concentration of closely associated active centres (VO_x clusters). This observation is in agreement with the well-known "site-isolation" theory [24–26]. This theory claims that a statistically controlled number of active sites favors selective oxidation reactions over combustion reaction. The dependence of propene yield on oxygen partial pressure can support the conclusion on importance of vanadia distribution (Fig. 3). A change of propene yield with increasing oxygen partial pressure depends on the catalytic material. Fig. 9 presents the dependence of the change of propene yield on the Mg/V ratio. The propene yield increases more strongly on materials with a high Mg/V ratio on an increase in oxygen partial pressure from 15 to 20 kPa.

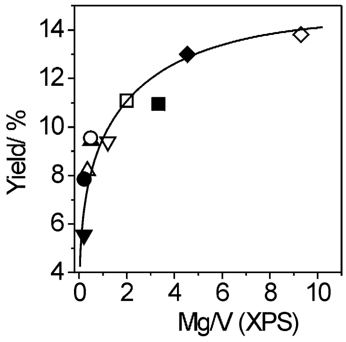

Fig. 8. Propene yield versus the Mg/V ratio determined by XPS ($C_3H_8/O_2/N_2 = 40/20/40$, $T = 773$ K, $X(O_2) \sim 100\%$): (■) $V_{0.3}Mg_{0.63}Ga_{0.07}$; (□) $V_{0.22}Mg_{0.47}Mo_{0.11}Ga_{0.2}$; (●) $V_{0.16}Mg_{0.11}Mo_{0.17}Fe_{0.09}Ga_{0.47}$; (○) $V_{0.32}Mg_{0.18}Mo_{0.04}Mn_{0.19}Ga_{0.27}$; (▲) $V_{0.2}Mg_{0.5}Ga_{0.3}$; (△) $V_{0.2}Mg_{0.2}Ga_{0.6}$; (▼) $V_{0.8}Mg_{0.2}$; (▽) $V_{0.5}Mg_{0.5}$; (◆) $V_{0.2}Mg_{0.8}$; (◇) $V_{0.1}Mg_{0.9}$.

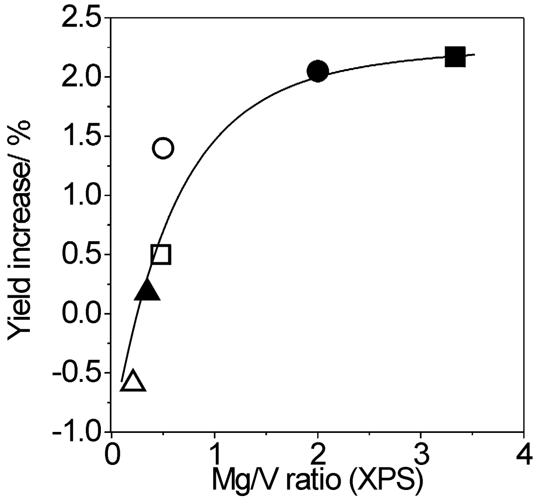

Fig. 9. Increase of propene yield versus the Mg/V ratio determined by XPS when propane/oxygen ratio is increased from 3 to 2: (■) $V_{0.22}Mg_{0.47}Mo_{0.11}Ga_{0.2}$; (●) $V_{0.3}Mg_{0.63}Ga_{0.07}$; (△) $V_{0.16}Mg_{0.11}Mo_{0.17}Fe_{0.09}Ga_{0.47}$; (□) $V_{0.32}Mg_{0.18}Mo_{0.04}Mn_{0.19}Ga_{0.27}$; (▲) $V_{0.2}Mg_{0.2}Ga_{0.6}$; (○) $V_{0.2}Mg_{0.5}Ga_{0.3}$.

From all the above results discussed it can be derived that a good catalytic performance for ODP is achieved by an optimal concentration of the active VO_x species which have to be well dispersed on the surface of effective catalytic materials.

This conclusion was ascertained by using high-surface area meso-porous siliceous MCM-48 and MCM-41 on which vanadia is well dispersed and stabilised as isolated vanadia species; this has been proven by ^{51}V solid state NMR, EPR, UV-Vis spectroscopy and TPR [14]. The catalytic performance data of VO_x (2.8 wt.%)/MCM-48 and VO_x (2.8 wt.%)/MCM-41 are presented in Table 4.

Table 4
Catalytic performance of VO_x/MCM catalysts in the ODP ($T = 773\,K$)

$C_3H_8/O_2/N_2$	m (g)	F (ml/min)	τ ($s\,g_{cat}\,cm^{-3}$)	$X(C_3H_8)$ (%)	$S(C_3H_6)$ (%)	$S(CO)$ (%)	$S(CO_2)$ (%)	$S(CH_4)$ (%)	$S(C_2H_4)$ (%)	$Y(C_3H_6)$ (%)
VO_x (2.8 wt.%)/MCM-41										
30/25/45	0.1	150	0.04	44.6	32.7	33.7	8.5	9.5	15.6	14.6
30/20/50	0.1	150	0.04	34.2	42.3	32.8	8.6	5.8	10.6	14.5
40/20/40	0.1	150	0.04	30.3	49.1	25.7	7.1	7.4	10.6	14.9
VO_x (2.8 wt.%)/MCM-48										
30/25/45	0.2	150	0.08	46.6	34.6	27.9	9.4	8.9	19.2	16.1
30/20/50	0.2	150	0.08	37.3	45.8	26.8	10.1	6.7	10.7	17.1
40/20/40	0.2	150	0.08	32.8	53.0	20.8	8.0	7.1	11.1	17.4

Using different propane/oxygen ratios it was possible to reach a maximal propene yield of 17.4%. These results confirm our above assumption that the catalytic performance is improved by a high dispersion of the isolated VO_x species.

5. Conclusions

For the identification of catalytic active materials and their further development for the ODP which was used as a model reaction for illustration it could be shown that the input of fundamental knowledge in the only seemingly empirical process of high-throughput synthesis and testing of materials for catalysis is a valuable method to develop new catalytic materials or to improve existing compositions. Fundamental knowledge supports the design of a 1st generation of materials to start with; this does not necessarily exclude to provide for the unexpected. Further, the characterisation of best performing materials identified in subsequent materials generations leading to fundamental insight was shown to give additional hints for improvement of the catalytic material. The more fundamental insights from a multitude of catalytic results are in agreement with earlier findings, in particular with respect to the isolated-sites concept.

Acknowledgements

The authors thank Mrs. R. Jentzsch for most of the catalyst preparation and catalytic experiments, Dr. M. Schneider for XRD analysis, Dr. J. Radnik for XPS measurements and Dr. H. Berndt for providing the VO_x (2.8 wt.%)/MCM-48 and VO_x (2.8 at.%)/MCM-41 materials. The work was supported by the German Federal Ministry for Education and Research and the Department of Science of the State of Berlin.

References

[1] D. Wolf, O.V. Buyevskaya, M. Baerns, Appl. Catal. A 200 (2000) 63.
[2] O.V. Buyevskaya, D. Wolf, M. Baerns, Catal. Today 62 (2000) 91.
[3] P.G. Schultz, X. Xiang, I. Goldwasser, Symyx technologies WO 96/11878, 1996.
[4] E. Danielson, J.H. Golden, E. McFarland, C.M. Reaves, W.H. Weinberg, X.D. Wu, Nature 389 (1997) 944.
[5] E. Reddington, A. Sapienza, B. Gurau, R. Viswanathan, S. Sarangapani, E.S. Smotkin, T.E. Mallouk, Science 280 (1998) 1735.
[6] S.M. Senkan, Nature 394 (1998) 350–352.
[7] S. Senkan, K. Krantz, S. Ozturk, V. Zengin, I. Onal, Angew. Chem. 111 (1999) 2965.
[8] H.H. Kung, Adv. Catal. 40 (1994) 1.
[9] E.A. Mamedov, V.C. Corberan, Appl. Catal. A 127 (1995) 1.
[10] Y. Moro-oka, W. Ueda, Catalysis, Vol. 11, Specialist Periodical Reports, Royal Society of Chemistry, Cambridge, UK, 1994 (Chapter 6).
[11] F. Cavani, F. Trifiro, Catal. Today 24 (1995) 307.
[12] M.A. Banares, Catal. Today 51 (1999) 319.
[13] P. Rybarczyk, H. Berndt, J. Radnik, M.-M. Pohl, O.V. Buyevskaya, M. Baerns, A. Brückner, J. Catal., accepted.
[14] H. Berndt, A. Martin, A. Brückner, E. Schreier, D. Müller, H. Kosslick, G.-U. Wolf, B. Lücke, J. Catal. 191 (2000) 384.
[15] M. Puglisi, F. Arena, F. Frusteri, V. Sokolovskii, A. Parmaliana, Catal. Lett. 41 (1996) 41.
[16] G. Centi, S. Perathoner, F. Trifitó, J. Phys. Chem. 96 (1992) 2617.
[17] M. Niwa, Y. Murakami, J. Catal. 76 (1982) 9.
[18] A. Brückner, A. Martin, B. Kubias, B. Lücke, J. Chem. Soc., Faraday Trans. 2221 (1998) 94.
[19] M. Morey, A. Davidson, H. Eckert, G. Stucky, Chem. Mater. 8 (1996) 486.
[20] M. Wark, A. Brückner, T. Liese, W. Grünert, J. Catal. 175 (1998) 48.
[21] M. Chaar, D. Patel, H.H. Kung, J. Catal. 109 (1988) 463.
[22] D.S.H. Sam, V. Soenen, J.C. Volta, J. Catal. 123 (1990) 132.
[23] A.G. Ruiz, I.R. Ramos, J.L.G. Fierro, V. Soenen, J.M. Herrmann, J.C. Volta, Stud. Surf. Sci. Catal. 72 (1992) 203.
[24] J.L. Callaham, R.K. Grasselli, AIChE J. 9 (1963) 755.
[25] Y. Morooka, Y. Morikawa, A. Ozaki, J. Catal. 7 (1967) 23.
[26] P.J. Andersen, H.H. Kung, Proceedings of the 10th International Congress on Catalysis, Paper O4, Budapest, 1992.